

M. Mulansky · K. Ahnert · A. Pikovsky and
D. L. Shepelyansky

Strong and weak chaos in weakly nonintegrable many-body Hamiltonian systems

March 14, 2011

Abstract We study properties of chaos in generic one-dimensional nonlinear Hamiltonian lattices comprised of weakly coupled nonlinear oscillators, by numerical simulations of continuous-time systems and symplectic maps. For small coupling, the measure of chaos is found to be proportional to the coupling strength and lattice length, with the typical maximal Lyapunov exponent being proportional to the square root of coupling. This strong chaos appears as a result of triplet resonances between nearby modes. In addition to strong chaos we observe a weakly chaotic component having much smaller Lyapunov exponent, the measure of which drops approximately as a square of the coupling strength down to smallest couplings we were able to reach. We argue that this weak chaos is linked to the regime of fast Arnold diffusion discussed by Chirikov and Vecheslavov. In disordered lattices of large size we find a subdiffusive spreading of initially localized wave packets over larger and larger number of modes. The relations between the exponent of this spreading and the exponent in the dependence of the fast Arnold diffusion on coupling strength are analyzed. We also trace parallels between the slow spreading of chaos and deterministic rheology.

Keywords Lyapunov exponent · Arnold diffusion · chaos spreading

PACS 05.45.-a · 05.45.Pq · 63.10.+a

1 Introduction

Even 120 years after the fundamental work of Poincaré [1] and numerous efforts done after it, an interplay between order and chaos in high-dimensional Hamiltonian systems remains a challenging problem. For Hamiltonian dynamics with a few degrees of freedom, a clear picture of a separation between chaotic and regular (quasiperiodic) regions in the phase space [2,3] has been confirmed in numerous studies. Much less is known on this separation and the structural properties of chaos when the number of degrees of freedom becomes large. Especially the generic case of a weak nonlinear coupling of initially nonlinear but integrable degrees of freedom remains poorly understood. We will call such systems to be weakly nonintegrable. Their properties are very nontrivial since a decrease in nonlinearity/nonintegrability might be compensated by an increase of dimensionality of the phase space.

The Kolmogorov-Arnold-Moser (KAM) theory guarantees the existence of invariant tori at a sufficiently weak nonlinear perturbation (see e.g. [2,3]). However, in conservative systems with more than

M. Mulansky, K. Ahnert and A. Pikovsky
Department of Physics and Astronomy, Potsdam University, Karl-Liebknecht-Str 24, D-14476, Potsdam-Golm, Germany

D. L. Shepelyansky
Laboratoire de Physique Théorique du CNRS (IRSAMC), Université de Toulouse, UPS, F-31062 Toulouse, France

two degrees of freedom ($L > 2$) such tori are not isolating and chaos can spread along tiny chaotic layers as it was pointed out by Arnold [4]. The mechanism of such a chaotic spreading is known under the name of Arnold diffusion as coined by Chirikov in 1969 [2,5]. For $L = 3$ the rate of Arnold diffusion drops exponentially with the dimensionless strength of nonlinear coupling β [2,3,5]. This is in a qualitative agreement with a number of mathematical results which give rigorous bounds on the spreading rate in the limit of asymptotically small β at fixed $L > 2$ [6,7]. The mathematical studies of the Arnold diffusion properties are actively continued at present (see e.g. [8] and Refs. therein). While the mathematical results indicate the exponentially small rate of Arnold diffusion D_A in the limit of small nonlinearity β at fixed L , it remains not clear at what realistic values of nonlinearity such an exponential behavior effectively appears. The striking results of Chirikov and Vecheslavov, established by extensive numerical simulations for $4 \leq L \leq 15$ and supported by heuristic arguments [9,10,11], show only an algebraic decay of D_A with β up to extremely small values of Arnold diffusion coefficient $D_A \sim 10^{-50}$. This regime was named by them the fast Arnold diffusion. These studies have been restricted by $L \leq 15$ and it remains unclear what can happen with such a behavior in the limit of larger L with small but fixed β .

The question about the properties of Hamiltonian systems at large values of L is linked to the fundamental problem of dynamical thermalization and ergodicity in the thermodynamic limit. As typical models with a large number of degrees of freedom one considers Hamiltonian lattices (or Hamiltonian partial differential equations, which, however, live in an infinite-dimensional phase space). A striking example of nontrivial dynamics in weakly nonlinear lattices gives the Fermi-Pasta-Ulam problem [12], which is still far from being completely resolved despite of numerous efforts in its 50-year history (see [13,14] for a stand around 2004 and [15] for recent advances). Moreover, because the FPU model has a special peculiarity as being close to an integrable Toda lattice, its properties appear to be rather special. Quite recently, a lot of attention attracted disordered nonlinear lattices [16,17,18,19,20,21,22,23,24,25,26,27] studied in the context of the problem of nonlinear destruction of Anderson localization. Here one tries to relate the properties of chaos and regularity at small nonlinearities to the properties of the spreading of a wave packet over the lattice [28,29,30]. Certain mathematical bounds on the rate of spreading have been obtained [31,32] by the methods similar to those of Nekhoroshev [6] but they are available only in the limit of very small nonlinearity being very far from the regimes studied in numerical simulations. In addition, these weakly nonlinear lattices are not generic objects from the point of view of weak nonintegrability and the KAM theory, since in the limit of small coupling they are reduced to a set of linear modes, i.e. to a linear quasiperiodic state demonstrating quasiperiodicity and pure point spectrum typical of the Anderson localization, and not to the generic case with a set of uncoupled *nonlinear* modes. We note, that in context of the KAM theory, a small perturbation of the latter integrable nonlinear system is studied.

In this paper we study properties of a lattice of weakly coupled nonlinear oscillators at small coupling and large number of degrees of freedom. In the limit of small coupling this model reduces to an integrable although strongly nonlinear one, demonstrating typically quasiperiodic dynamics. A nice model of such a setup has been suggested by Kaneko and Konishi [33,34], it gives a generalization of the Chirikov standard map [2] to a lattice of coupled symplectic maps. This model is computationally efficient and allows one a rather good numerical characterization of properties of regular and chaotic dynamics. Nevertheless, even for this model the quantitative properties are not well-established despite of various efforts [35,36,10,11,37]. Additionally, we study here two models of coupled nonlinear continuous-time oscillator lattice where the spreading over the lattice can be analyzed at fixed energy. Our main conclusions are valid for all these systems.

The plan of the paper is as follows. We start by formulating basic models we study in Section 2. Then in Section 3 we discuss the properties of the largest Lyapunov exponent, especially the scaling relations in dependence on coupling strength and system length. In Section 4 we argue that chaos is mainly due to occasional resonances between triples of three neighboring oscillators. In Section 5 we discuss statistical properties of chaos, focusing on the scaling of the diffusion constant. In Section 6 we relate this properties to that of spreading of a wave packet in an unbounded lattice. Finally, in Section 7 a very slow evolution is compared to similar effects in the context of rheology.

2 Basic models

Here we introduce three generic models of nonlinear oscillators locally coupled in space. Model A, introduced by Kaneko and Konishi [33,34], is a model of coupled symplectic maps

$$\begin{aligned}\bar{p}_k &= p_k + K[\sin(x_{k+1} - x_k) + \sin(x_{k-1} - x_k)], \quad k = 1, \dots, L \\ \bar{x}_k &= x_k + \bar{p}_k.\end{aligned}\tag{1}$$

with periodic boundary conditions. Here p is a ‘‘momentum’’ and x is a ‘‘phase’’ variable. In the absence of coupling (i.e. for $K = 0$) each oscillator has a constant frequency p_k that depends on initial conditions, so in the whole lattice generally a quasiperiodic regime with L frequencies establishes. For finite K the oscillators are coupled and chaos is possible.

Model B is a strongly nonlinear continuous-time lattice with Hamiltonian

$$H = \sum_{k=1}^L \frac{p_k^2}{2} + \frac{q_k^4}{4} + \frac{\beta}{2}(q_{k+1} - q_k)^2.\tag{2}$$

Here we also consider a lattice of length L with periodic boundary conditions. The coupling parameter β plays the same role as K . Contrary to model A, model B conserves the total energy. We normalize the energy in such a way that $E = L$ (i.e. density of energy is one), so that β and L are the only parameters of this model.

Very similar to the model B is the model C, where the coupling between nonlinear modes is also nonlinear, moreover, the power of nonlinearity in coupling is stronger than the local one:

$$H = \sum_{k=1}^L \frac{p_k^2}{2} + \frac{\eta_k q_k^4}{4} + \frac{\gamma}{6}(q_{k+1} - q_k)^6,\tag{3}$$

where we consider two cases for coefficients with all $\eta_k = 1$ (C1) and random homogeneously distributed values $0.5 \leq \eta_k \leq 1.5$ (C2). While we do not expect large difference between models B and C in the described setup, where the density of the energy is fixed, the situation changes when the total energy is fixed and the length of the lattice is increased. In this limit model B will become asymptotically linear (effective β increases) while model C will become asymptotically less and less coupled (effective γ decreases). This difference is important for the implications of chaos for spreading of initially localized wave packets, to be discussed in Section 6. The randomness of values of η_k (model C2) ensures that there are no regular waves emanating from the main part of the wave packet in contrast to the case $\eta_k = 1$ (model C1) where such wave radiation is possible [39,40].

3 Lyapunov exponents and their scaling

3.1 Lyapunov exponents

The largest Lyapunov exponent (LE) is a standard measure of chaos and is easy to calculate [3,38]. We have performed a statistical analysis of Lyapunov exponents for models A, B, C based on an ensemble of random initial conditions. For model A we have chosen $0 \leq p_k, x_k < 2\pi$ as independent uniformly distributed. For model B we initialized $q_k = 0$ and p_k normally distributed with zero mean, after this the values p_k are rescaled such that the total energy of the lattice equals L - the number of lattice sites. For the model C the initialization is done in a similar way. We used up to several thousands of initial state realizations to obtain a good statistics in the computation of measure of chaos P_{ch} .

We present the ‘‘raw data’’ of these calculations for models A and B in Fig. 1. Here, for model A in a lattice with $L = 8$ one observes predominantly chaos for $K = 0.05$, predominantly regularity for $K = 0.001$, and both states depending on initial conditions for $K = 0.01$. Noteworthy, LE in the case of regularity does not vanish but attains very small values, with the cutoff appearing due to a finite integration time. In the middle part of Fig. 1(a) one can see that increasing the integration time by factor 10 roughly decreases this lower cutoff in the Lyapunov exponent by factor 10. For any fixed T_{av} , basing on inspection, one easily chooses a threshold in LE that separates chaos from regularity. Of

course, there are realizations with values around these thresholds that cannot be resolved within the integration time used, but their statistical relevance is not significant. Essentially the same picture is observed for models B (Fig. 1b) and model C (data not shown).

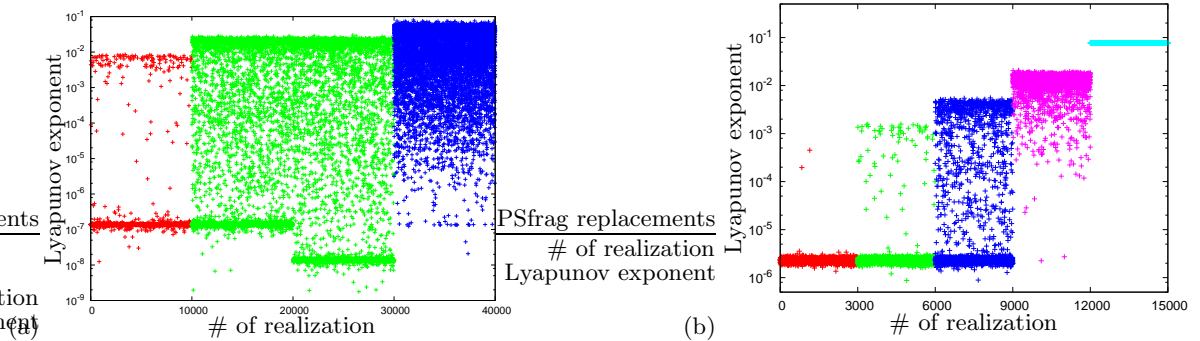


Fig. 1 (Color online) (a) Calculations of LEs for model A with $L = 8$. First 10000 points (red): $K = 0.001$, LE calculated by averaging over time interval $T_{av} = 5 \cdot 10^6$. Second 10000 points (green): $K = 0.01$, $T_{av} = 5 \cdot 10^6$. Next 10000 points (also green): $K = 0.01$, $T_{av} = 5 \cdot 10^7$. Last 10000 points (blue): $K = 0.05$, $T_{av} = 5 \cdot 10^6$. (b): The same as (a) but for model B with $L = 16$, $T_{av} = 10^6$ and different β , from left to right: $\beta = 10^{-5}, 10^{-4}, 10^{-3}, 10^{-2}, 10^{-1}$, for each value of β 3000 realizations are shown.

3.2 Scaling of probability to observe chaos

According to calculations of LEs we can distinguish chaotic and regular regimes, and calculate the probability of their appearance in models A, B, C. The results for coupled symplectic maps of model A are presented in Fig. 2. A typical lower cutoff for the LE calculated over time interval $T = 10^8$ was $\approx 2.5 \cdot 10^{-8}$, so we attributed all the realizations with $\lambda > 5 \cdot 10^{-7}$ to chaos. Defined in this way the total measure of initial conditions in the phase space that yield chaos P_{ch} decreases with K and L . The rescaled plot shows that for small K and large L the scaling relation

$$P_{ch} \sim K \cdot L \quad (4)$$

holds. The same scaling $P_{ch} \sim K \cdot \beta$ is valid also for model B, as demonstrated in Fig. 3, and for model C (Fig. 4).

The scaling with the system length $P_{ch} \sim L$ has been already discussed for model A in [35, 36] and for disordered nonlinear lattices in [30]. It is based on the locality of chaos: the latter appears due to a local in space nonlinear interaction of localized modes, and not due to propagation of waves. Thus, in order to observe regularity in the whole lattice, the dynamics has to be regular in all subparts. Therefore, if the measure of chaos in a sublattice of length L_0 , $P_{ch}(L_0)$, is small, then $P_{ch}(L) \approx 1 - (1 - P_{ch}(L_0))^{L/L_0}$ from which the scaling $\log P_{ch} \sim L$ follows. An additional check of this relation is in Fig. 5b below.

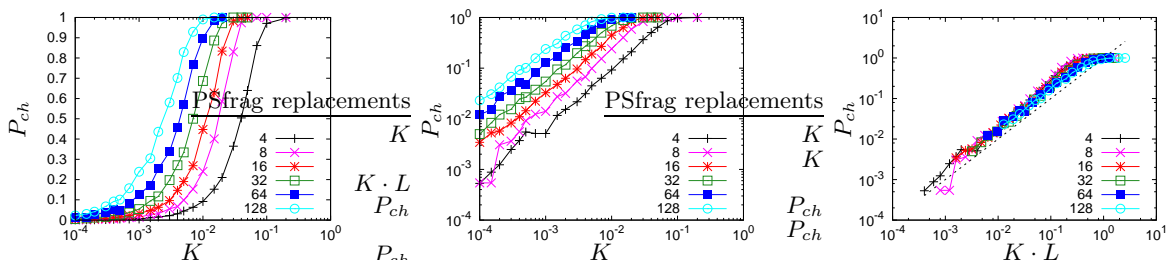


Fig. 2 Calculations of P_{ch} vs K for model A, demonstrating the scaling $P_{ch} \sim KL$ for small K . The middle panel shows the same data as the left one but in a logarithmic scale, while the left panel shows P_{ch} as a function of the product KL . The dashed line on the right panel is $P_{ch} = KL$.

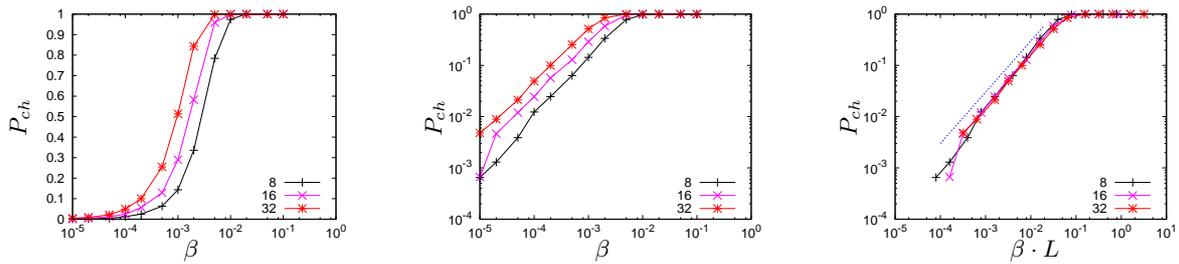


Fig. 3 The same as Fig. 2 but for model B.

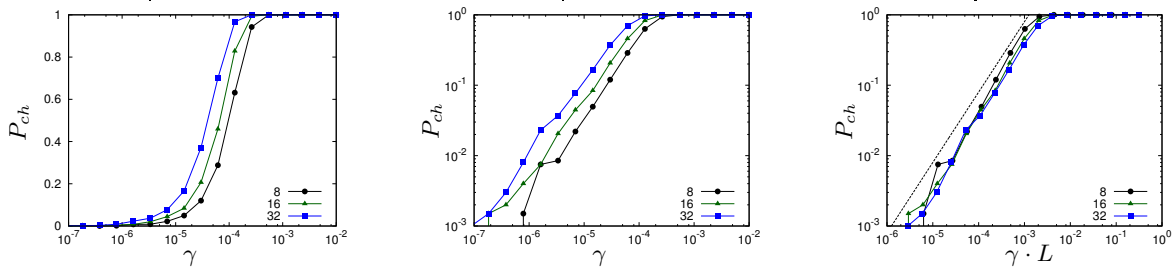


Fig. 4 The same as Fig. 3 but for model C1.

3.3 Scaling of the Lyapunov exponent

Next, we studied the scaling properties of the value of LE. As one can already see from Fig. 1, the positive LEs concentrate around a maximal value that decreases with K and β . We have found (see Fig. 5a) that this maximal value is roughly independent on the length of the system L and scales with nonlinearity parameters K and β as

$$\lambda \sim K^{1/2}. \quad (5)$$



Fig. 5 Left panel: Dependence of the Lyapunov exponent λ on the perturbation parameter K for model A at $L = 4$ (blue circles), 8 (red squares). Dashed straight line shows approximate dependence $\lambda = 0.16\sqrt{K}$ (for $N = 4, 8$). The fit of data gives the exponent of the dependence $\lambda \propto K^a$ with $a = 0.476 \pm 0.013$ (for $L = 4$), 0.450 ± 0.012 (for $L = 8$) in agreement with the scaling (5). Right panel: Dependence of the measure of chaos P_{ch} on the perturbation parameter K for $L = 4$ (blue circles), 8 (red squares). Dashed straight line shows approximate dependence $P_{ch} = 7.75K$ (for $L = 4$); for $L = 8$ we find that $P_{ch} = 14.32K$ in agreement with the scaling (4). The fit of data gives the exponent of the dependence $P_{ch} \propto K^b$ with $b = 1.022 \pm 0.01$ (for $L = 4$), 1.036 ± 0.01 (for $L = 8$). Up to 5×10^5 trajectories and time $t \leq 10^6$ have been used to compute the Lyapunov exponent λ and determine the number of chaotic trajectories with $\lambda > 0$. Certain checks have been made with $t = 5 \times 10^9$ and 100 trajectories.

To demonstrate the scaling of the Lyapunov exponents we calculated their probability distribution densities $w(\lambda)$. Because of the relation $P_{ch} = \int_{\lambda_{th}}^{\infty} w(\lambda) d\lambda$ (where λ_{th} is the cutoff value) the appropriate scaling for this density is that of P_{ch} , i.e. $K \cdot L$. According to (5), the appropriate scaling of

the argument of the density is $\lambda K^{-1/2}$. We plot rescaled in this way distribution densities of LEs for models A and B in Figs. 6 and 7. We present here results for the distribution density w , for constructing of which some arbitrary bins have been used, and for a cumulative distribution $W(\lambda) = \int_{\lambda}^{\infty} w(\lambda) d\lambda$ where all data are presented, respectively. We note that the scaling law (5) differs from the scaling $\lambda \sim K^{2/3}$ suggested in [35,36]. For the model B we find the same scaling relation $\lambda \sim \beta^{1/2}$ as it is shown in Fig. 7b. For the model C we find the similar relation.

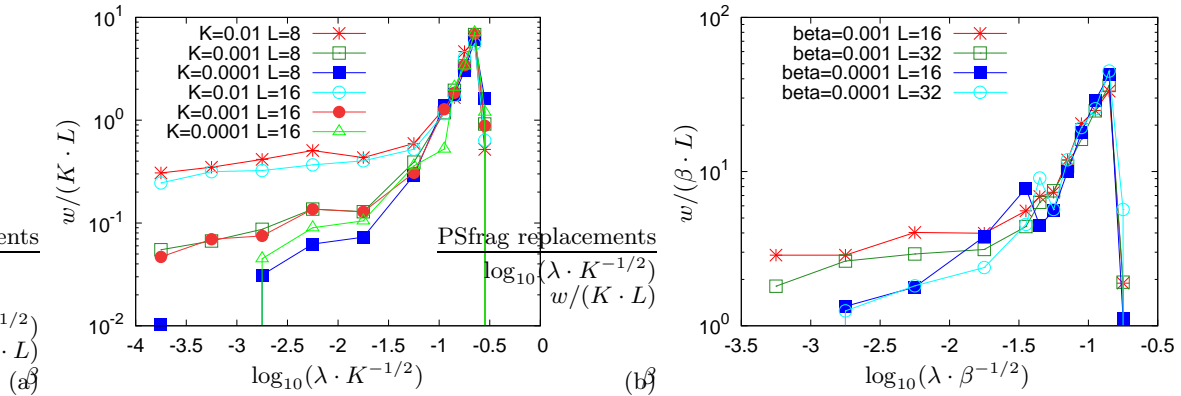


Fig. 6 (a): Distribution density of LEs in model A. (b): Distribution density of LEs in model B.

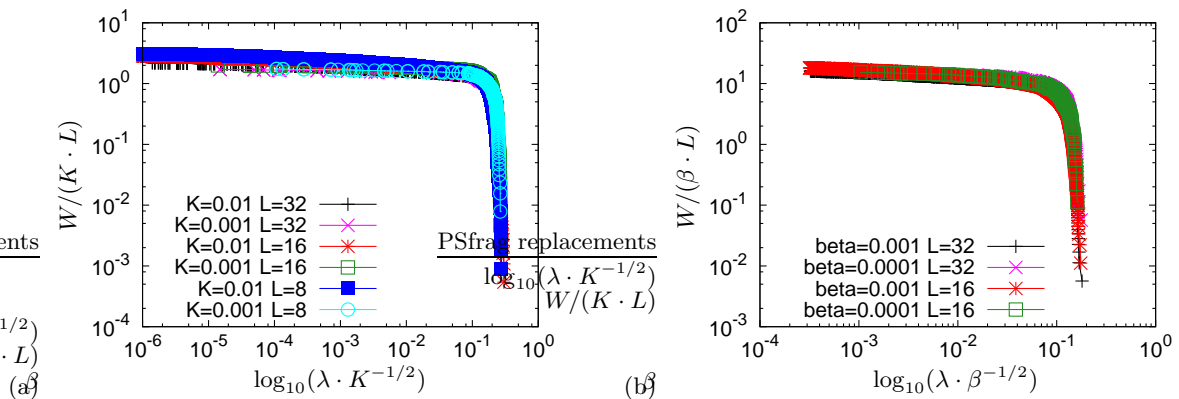


Fig. 7 (a): cumulative distribution of LEs in model A. (b): cumulative distribution of LEs in model B.

3.4 Strong and weak chaos

There is also a substantial part of trajectories that have LEs between the lowest cutoff (determined by the averaging time) and the largest value $\sim \sqrt{K}$. We will distinguish these regimes by referring to the dynamics with LEs in the peak of distribution in Fig. 6 as *strong chaos* while the dynamics with lower LEs will be called *weak chaos*. As it will be discussed later, it might be that the regime of weak chaos is that where the fast Arnold diffusion discussed in [11] occurs. We show in Fig. 8 that the total probability P_{wch} to observe this weak chaos scales as

$$P_{wch} \propto K^{\nu_{wch}} L, \quad \nu_{wch} \approx 1.6. \quad (6)$$

In Fig. 9 we show an example of a local in time LEs for one long trajectory in model A. It shows existence of transitions between regimes with strong chaos and weak chaos.

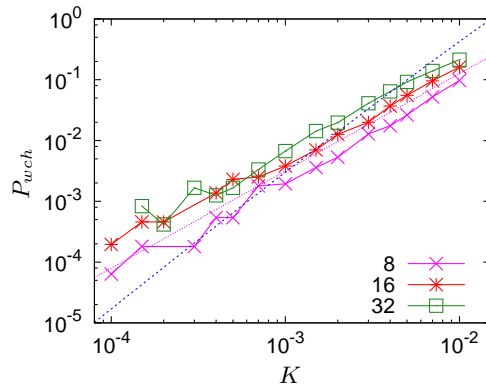


Fig. 8 Probability of “weak chaos” P_{wch} with the LE between the low $\lambda > 10^{-7}$ and high ($\lambda < 0.03 \cdot K^{1/2}$) cutoffs in Fig. 7 in model A. The pink dotted line is $P_{wch} \sim K^{1.6}$, the dashed curve corresponds to the estimate $P_{wch} \sim K^{2.5}(\ln K)^2$, discussed at the end of Section 5 in relation to the regime of fast Arnold diffusion analyzed in [11].

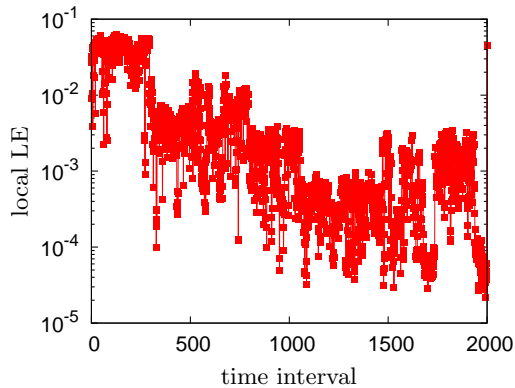


Fig. 9 Local LEs in model A as a function of time. Each value of LE is calculated over time interval of length 10^6 , here $2 \cdot 10^3$ such time intervals are shown; $K = 0.05$, $L = 8$.

4 Resonances as a source of chaos

In order to characterize conditions under which chaos occurs at very small coupling, we have looked on resonances, and have found that chaos is highly correlated with the triple resonance at which the frequencies of three neighboring oscillators nearly coincide. For models A and B we illustrate this in Figs. 10, respectively. Here the probability of chaos P_{ch} is shown vs. renormalized distances of initial frequencies of oscillators. For model A we have defined this distance as $d = \min_k [(f(p_k^{(0)} - p_{k+1}^{(0)}))^2 + (f(p_{k+1}^{(0)} - p_{k+2}^{(0)}))^2]$. Here $f(x) = 2|\sin 0.5x|$ measures the closeness of two initial momenta modulo 2π . A small value of d indicates that somewhere in the lattice three initial nearby momenta $p^{(0)}$ are close to each other. Then, for different realizations of initial conditions, different K in the range $[0.001, 0.2]$ and different lattice lengths $L = 8, 16, 32$ we determined the probability for chaos to occur vs. d/\sqrt{K} . One can see that for different lattice lengths the curves are close to each other, thus indicating that indeed the occurrence of resonances is a necessary prerequisite for chaos. In a similar analysis for model B we used $d^2 = \min_k [(\sqrt{p_k(0)} - \sqrt{p_{k+1}(0)})^2 + (\sqrt{p_k(0)} - \sqrt{p_{k-1}(0)})^2]$.

In Fig. 10 we demonstrate the correlation between the occurrence of resonance (small d) and the probability to observe chaos P_{ch} . Moreover, we see here the scaling that in fact d should be compared with \sqrt{K} (or $\sqrt{\beta}$ for model B).

The physical reason for the scaling results presented in previous sections is the following (for simplicity of presentation, we refer here to model A only, the same arguments work for models B and C). There is a finite probability that three nearby particles will have their frequencies $\omega_i = p_i$ close to each other, within the frequency range $\Delta\omega = \sqrt{K}$. The probability of such an event is $P \sim K$, since

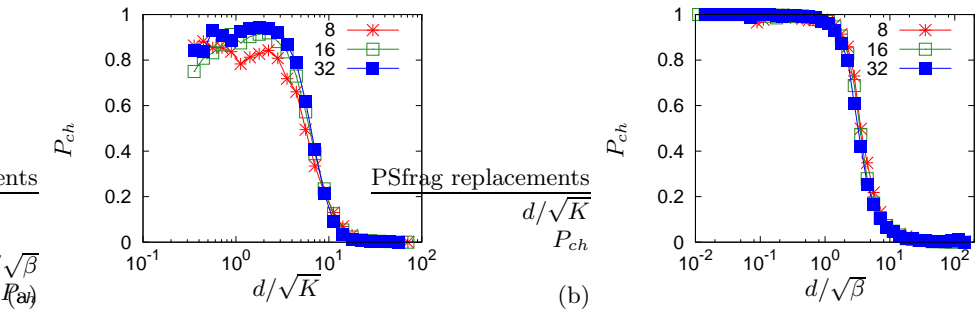


Fig. 10 The probability to observe chaos in dependence on the resonance in initial data for models A (a) and B (b). The data for different L and K, β collapse if the distance in initial frequencies is scaled according to \sqrt{K} or $\sqrt{\beta}$.

the first particle may have any frequency, the probability to have the second in the range \sqrt{K} is \sqrt{K} and the probability to have the third in the same range is also \sqrt{K} . This gives the probability of the resonance $P \sim K$ for a lattice with three particles and $P \sim KL$ for a chain with L oscillators. Similar arguments work for models B, C. It is important to note that in the case of such a 3-particle resonance, the KAM arguments are not valid and the dynamics remains chaotic at arbitrary small perturbation K . The situation is similar to the one considered in [41] where three linear oscillators with the same frequency remain chaotic at arbitrary small nonlinear coupling between them. Indeed, in our case the numerical analysis shows that almost all chaotic trajectories (those with positive Lyapunov exponent) have three nearby particles with close frequencies.

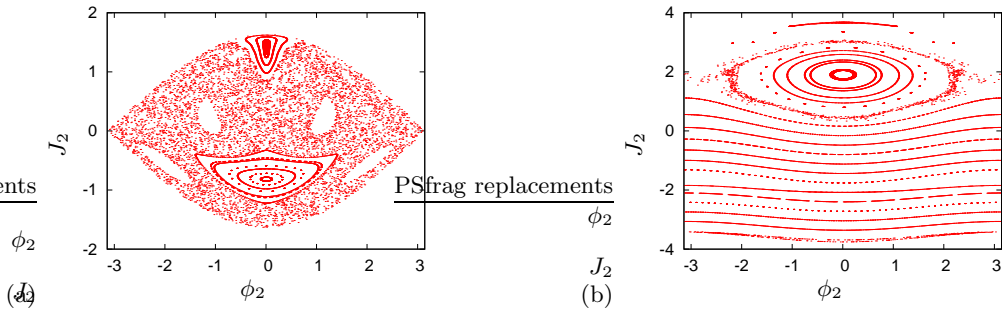


Fig. 11 Poincaré sections of variables ϕ_2, J_2 for the resonance Hamiltonian (12) at $\phi_1 = 0$. (a): $H_R = 0$, here chaos is dominant. (b): $H_R = 10$, here the dynamics is typically quasiperiodic.

To understand this phenomenon in a better way let us consider the case when initially at three neighboring sites the values of actions p_i are close to their average value $P = (p_1 + p_2 + p_3)/3$. Then the evolution of these three particles, considered separately from the rest (what can be justified by arguing that nonresonant terms effectively disappear after averaging) is described by the mapping

$$\bar{p}_1 - p_1 = K \sin(x_2 - x_1), \quad \bar{x}_1 - x_1 = \bar{p}_1, \quad (7)$$

$$\bar{p}_2 - p_2 = K \sin(x_1 - x_2) + K \sin(x_3 - x_2), \quad \bar{x}_2 - x_2 = \bar{p}_2, \quad (8)$$

$$\bar{p}_3 - p_3 = K \sin(x_2 - x_3), \quad \bar{x}_3 - x_3 = \bar{p}_3. \quad (9)$$

Exploring the integral $p_1 + p_2 + p_3 = \text{const}$ and performing a canonical transformation to new conjugate coordinates according to

$$\phi_1 = x_1 - x_2, \quad \phi_2 = x_3 - x_2, \quad \phi_3 = x_1 + x_2 + x_3, \quad p_1 = I_1 + I_2 + P, \quad p_2 = -I_1 - I_2 + I_3 + P, \quad p_3 = I_2 + I_3 + P,$$

we obtain a two-dimensional mapping

$$\bar{I}_1 - I_1 = -K \sin \phi_1, \quad \bar{\phi}_1 - \phi_1 = 2\bar{I}_1 + \bar{I}_2, \quad (10)$$

$$\bar{I}_2 - I_2 = -K \sin \phi_2, \quad \bar{\phi}_2 - \phi_2 = 2\bar{I}_2 + \bar{I}_1, \quad (11)$$

which due to smallness of I_1, I_2 and of K can be approximated as a continuous-time system with Hamiltonian $H = I_1^2 + I_2^2 + I_1 I_2 - K \cos \phi_1 - K \cos \phi_2$. After rescaling of actions to $J_i = I_i/\sqrt{K}$ and time to $\tau = \sqrt{K}t$ we come to dimensionless resonance Hamiltonian

$$H_R(J_1, J_2, \phi_1, \phi_2) = J_1^2 + J_2^2 + J_1 J_2 - \cos(\phi_1) - \cos(\phi_2) \quad (12)$$

Note that this rescaling proofs the dependencies $\sim K^{1/2}$ for the allowed deviations from the resonance condition. Also the rescaling of time proofs the scaling of the Lyapunov exponent with K according to (5).

According to the Chirikov resonance-overlap criterion [2] the dimensionless dynamics of Hamiltonian (12) is chaotic for small values of energy (i.e. close to resonance) and chaos disappears if the energy is large. The Poincaré sections for H_R for $H_R = 0$ and $H_R = 10$ are shown in Fig. 11 confirming this picture.

5 Properties of diffusion and weak chaos

While LEs serve as an important indication for chaos, other quantities like correlations are important to characterize irregularity of the dynamics. For the Chirikov standard map an important statistical quantity is the diffusion constant of the momentum p : at large times T the dynamics of p can be considered as a random walk with a diffusion constant D defined according to $\langle (p(T) - p(0))^2 \rangle = DT$. For the Chirikov standard map the dependence of D on the parameter K is known in detail [2,3].

For the coupled symplectic maps (model A) numerical computations [33,34], performed in a range $0.1 < K < 1$, indicated a weak diffusion at $K = 0.1$, the authors fitted the data with a stretched exponential dependence. Here we extend these calculations and show the results in Fig. 12. One can see a strong decrease of the diffusion constant with K , which for small K is close to a power-law dependence

$$D \sim K^{\nu_D}, \quad \nu_D \approx 6.5. \quad (13)$$

A similar value of the exponent was obtained from the statistics of Poincaré recurrences in the range $0.1 \leq K \leq 1$ [42]. We note that for model C the above equation implies $D \propto \gamma^{\nu_D}$. The value of the exponent ν_D is close to the value given by Chirikov and Vechevslavov [10,11]. However, they calculated the diffusion indirectly by expressing it via an effective width w_s of a separatrix layer of a nonlinear resonance with the additional relation $D \sim K^{3/2} w_s^2$, which was verified with the direct computations of the Arnold diffusion in systems with a few degrees of freedom. In fact, the value of w_s is determined in [10,11] via the computation of the period of oscillations around a separatrix layer of a nonlinear resonance that is related to the computation of LE. Due to this indirect method, Chirikov and Vechevslavov were able to obtain the variation of the Arnold diffusion constant D_A by 50 orders of magnitude! On a scale of first 30 orders of magnitude the decay of the diffusion constant D is well described by the power law with $\nu_D = 6.5$ (see Fig. 1 in [11]). The main message of these amazing calculations is a non-exponential decay of D , and hence of the chaos measure w_s , with the decrease of nonlinearity parameter K . This result is in a drastic difference from the asymptotic Nekhoroshev-like estimates based on the KAM theory [6,7] which give exponential decrease of D and w_s as $K \rightarrow 0$. Of course, there is no formal contradiction since the results for fast Arnold diffusion [11] are always obtained at small but finite K values. However, an algebraic decrease with K indicates on an existence of weak chaos component with relatively large measure. The heuristic arguments for this phenomenon were presented in [11]. According to the results of [11] one has for model A:

$$D \sim K^{3/2} w_s^2, \quad w_s \sim K^{\nu_s}, \quad \nu_s \approx 2.5, \quad \nu_D = 2\nu_s + 3/2, \quad (14)$$

for $K > 1.6 \cdot 10^{-5}$. Here, w_s is a dimensionless measure of the chaotic separatrix layer of the resonance between two nearby oscillators. For the range $2 \cdot 10^{-6} < K \leq 1.6 \cdot 10^{-5}$ the decay of D is compatible with the power law $D \propto K^{15}$ but this range of K variation is not very large. The global dependence $D(K)$ is fitted by the dependence of Eq. (5.8) in [11] which however has no complete theoretical explanation.

The reason why one can hardly compute the diffusion coefficient at smaller K is clear from the inspection of the dependence of the variance on time in Fig. 12. For small K one observes a normal diffusion only when the variance exceeds ≈ 1 , below this value the diffusion looks like anomalous one with the variance proportional to a power of time. This means that a “random walk” inside the

periodicity cell $[0, 2\pi)$ is highly correlated, while only cell-to-cell walk demonstrates a normal diffusion. For small K the mean first passage time to the next cell becomes extremely large – nearly 10^9 for $K = 0.03$, while for $K < 0.03$ this mean passage time is of order or larger than the total integration time and only the anomalous diffusion is observed.

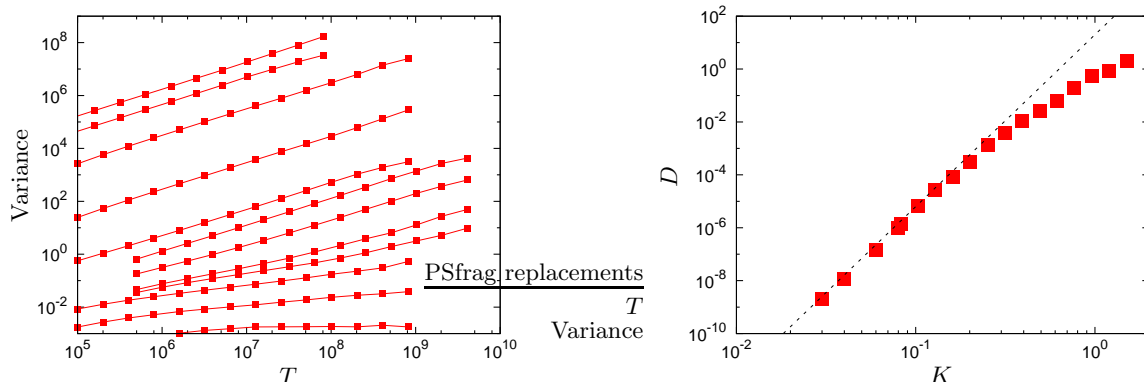


Fig. 12 Left panel: Variance $\langle (p(T) - p(0))^2 \rangle$ as a function of time T calculated in a lattice of length $L = 64$. From top to bottom: $K = 1.5, 1., 0.5, 0.2, 0.11, 0.08, 0.06, 0.05, 0.04, 0.03, 0.01, 0.005, 0.002$. Right panel: dependence of the diffusion constant on K in range $0.03 < K < 1.5$. Dashed line shows relation $D = 20K^{6.5}$.

The obtained properties of diffusion should be contrasted to the properties of LEs, as both quantities give some characteristic times of the system. We have demonstrated that these times become extremely different for small non-integrabilities, as the Lyapunov exponent $\lambda \sim K^{1/2}$ decreases rather weakly with K while the diffusion constant $D \sim K^{6.5}$ drops much more rapidly. We interpret this as indication that chaos is mainly “local”, not leading to large deviations of variables. This picture corresponds well to the discussed above effective resonances as the origin of chaos: in the triple resonance described above in Section 4, the sum of all momenta is a conserved quantity, so that the chaotic dynamics like in Fig. 11 does not lead to a large deviation of momenta involved in the resonance. Indeed, there is strong chaotic dynamics inside the triplet resonance, but the sum of three resonant actions is a constant in the resonance approximation that would give a zero diffusion coefficient $D = 0$. However, the resonant approximation is not exact and it is destroyed by nonresonant terms and higher order perturbations that leads to a finite value of the diffusion $D \sim K^{6.5}$. A mixture of strong chaos, which is however bounded due to an additional integral of motion, and a slow but unbounded diffusion produced by weak chaos makes the numerical computation of the diffusion rate a rather difficult task. In fact, usual very powerful methods discussed in [43], which allowed to compute as small diffusion rate as 10^{-22} , are not working in such a situation and only computations at very long times allow to determine directly the value of D .

The physical origins of the power law decay of the diffusion rate with K (13) are still to be understood. The theoretical heuristic arguments presented in [11] assume that in the regime of weak chaos a trajectory follows mainly those chaotic resonant layers which have locally most large size. An optimization over various resonances leads to a certain power law decay for w_s and D which gives $\nu_s = e = 2.718\dots$ and $\nu_D = 1.5 + 2e = 6.936\dots$ respectively (we remind that for the Chirikov standard map $w_s \propto \exp(-\pi^2/\sqrt{2K})$ [2,11]). This theoretical value of the exponent ν_D is in a satisfactory agreement with the numerical value found at not very small K values. However, at very small values of $K < 10^{-5}$ such arguments should be modified to fit an unknown dependence of resonance amplitudes in high orders of perturbation theory [11]. According to the heuristic arguments [11] the main contribution to diffusion is given by the resonances with an effective resonance harmonic numbers $\tilde{M}_0 = \ln(1/\sqrt{K})$ with a dimensionless measure of chaos inside one given resonance separatrix layer w_s . We may argue that the number of such layers grows with \tilde{M}_0 at least as \tilde{M}_0^2 so that the total measure of weak chaos can be estimated as $P_{wch} \propto \tilde{M}_0^2 w_s \propto (\ln K)^2 K^{2.5}$. This dependence is in a satisfactory agreement with the data of Fig. 8 (see the dashed curve there) and the empirical exponent value $\nu_{wch} \approx 1.6$ in (6). Thus we can say that our data for the measure of weak chaos are in a satisfactory agreement with the numerical results [11].

On the other hand, the origin of such a weak chaos component is still to be clarified. Indeed, the studies and arguments presented in [11] did not take into account the strong chaos based on triplet resonances which exists at arbitrary small K . This strong chaos component emerges as the result of triple primary resonances but it is clear that a similar mechanism can work for higher order resonances which may be at the origin of the weak chaos component. On the other hand, the triple-like resonances of higher order in K should lead to appearance of a certain number of trajectories with the LEs $\lambda \propto K^{m/2}$ with $m \geq 2$ that is, however, is not visible in the distribution of LEs in Figs. 6,7,8. It is however, possible that other tiny chaotic layers hide such contributions. Further studies are required to clarify these points especially in the regime with large $L \gg 15$. An indication on the complex internal structure of weak chaos provides Fig. 9 above, which demonstrates how a trajectory visits regions with different LEs along a very long evolution.

6 Spreading of chaos

Above we discussed the local properties of chaos computing the Lyapunov exponents and the diffusion rate in the regime when all nonlinear oscillators are populated in the initial state. Another type of question appears for the model C2 (3) when only one of few nearby oscillators are initially excited with the total energy $E_{tot} = 1$ and $\gamma = 1$ while all other oscillators have zero energy. Since the total energy is conserved we face the question on a possibility of energy spreading over the whole lattice of size L . This is related to the question of ergodicity of large finite lattices at small energies. In the case when both nonlinear terms in the Hamiltonian (the local potential and the coupling) have the same power (e.g. the coupling has power 4 instead of 6, such a model can be called model C44) then it is known that a thermalization takes place at arbitrary small total energy according to the arguments given in [40]. Of course, the time for such global ergodicity grows as a power of system size L . For models with a nonlinear destruction of the Anderson localization, we have the terms with powers 2 for local potential and 4 for coupling in (3), which we call model C24. In this case it is found that a slow subdiffusive spreading over the lattice takes place up to very long times $t \sim 10^9$ (see details in recent papers [18, 19, 20, 24, 25, 26, 27, 29, 40]). The model C2 corresponds to a new situation for energy spreading when the unperturbed integrable Hamiltonian is nonlinear and the coupling between nonlinear modes has higher nonlinearity. In contrast to the FPU problem, here the coupling between modes is local and the randomness in local nonlinear frequencies η_k excludes any proximity to a full hidden integrability.

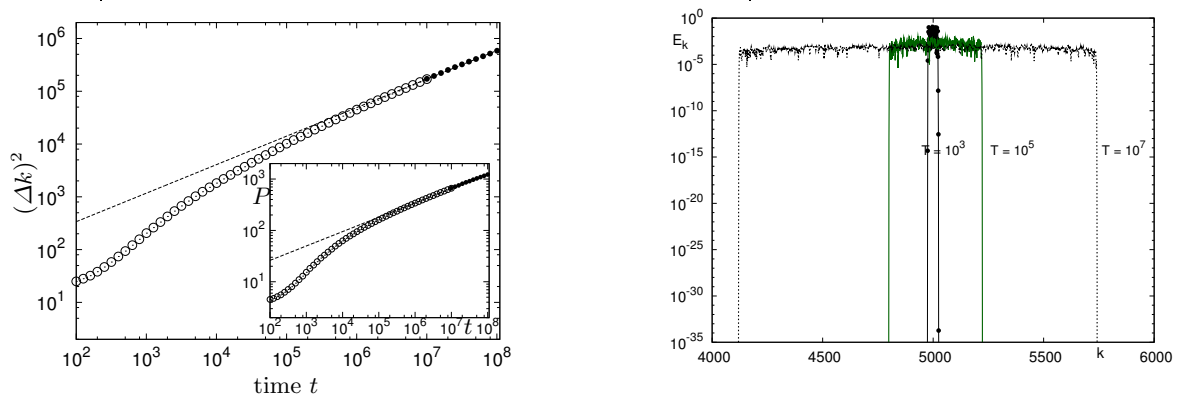


Fig. 13 Left panel: Spreading of the second moment $(\Delta k)^2 = \sum_k (k - k_0) E_k / \sum_k E_k$ and participation number $P = (\sum_k E_k)^2 / \sum_k E_k^2$ (inset) vs. time for initial single site excitation $k_0 = 0$ in model C2. Data up to $t = 10^7$ (empty circles) has been averaged over 1000 realizations of disorder and logarithmic time windows. Long-time values until $t = 10^8$ (full circles) were averaged over 24 realizations. Dashed lines show subdiffusive growth $(\Delta k)^2 \sim t^\alpha$ and $P \sim t^{\alpha/2}$ where the fit of the asymptotic behavior ($t > 10^5$) gave $\alpha = 0.55 \pm 0.01$. Right panel: energy distribution E_k in model C2 at certain moments of time $t = 10^3, 10^5, 10^7$ for one specific realization of disorder.

Let us assume that in model C2 with the above local initial conditions the energy spreads over the whole lattice of L oscillators with an approximate energy equipartition over L sites. After a rescaling of variables of this final state to a new time $\tau \rightarrow L^{1/4}t$ we come to the model C2 with $\gamma \sim 1/\sqrt{L}$ and a homogeneous initial condition, discussed in the previous sections. In general, the probability of strong chaos in such a case scales as $P_{ch} \propto \gamma L \propto \sqrt{L}$ so that we expect local strong chaos to occur almost surely in a sufficiently long lattice. The same is true for the probability of weak chaos even if in this case the sum value of the exponents in L is close to zero. Although the probability to observe chaos is high, it is important to note that this chaos is mainly local: some modes are chaotic, e.g. triplets discussed above, but other modes generally oscillate nearly quasiperiodically. Indeed, in a system with many degrees of freedom some modes can be chaotic while others can be close to integrable ones, without any contribution to the maximal LE. Thus, it is not obvious if the local strong chaos can allow spreading from initial local state over the whole lattice.

Let us present here simple estimates on the possible rate of such a spreading using results for the diffusion in the weak chaos component. We assume that a chaotic spreading populates the number of modes N at time t . Using rescaling given above we can argue that the new mode $N + 1$ will be populated due to the weak chaos diffusion after a time scale $t_s/N^{1/4} \sim 1/D(\gamma) \sim \gamma^{-\nu_D} \sim N^{\nu_D/2}$. This gives us an effective local diffusion rate in N with $N^2/t \sim 1/t_s \sim 1/N^{(2\nu_D+1)/4}$ leading to the subdiffusive growth of the second moment N^2 :

$$N^2 \sim t^\alpha, \quad \alpha = 8/(9 + 2\nu_D). \quad (15)$$

For $\nu_D = 6.5$ we obtain $\alpha = 0.3636$. However, our results for spreading, shown in Fig. 13, give approximately $\alpha = 0.55$ that corresponds to $\nu_D \approx 2.77$. We explain this difference in the following way. At the maximum time $t_{max} = 10^8$, reached in our numerical simulations, the energy spreads over a number of modes $N \sim t_{max}^{\alpha/2}$ so that we have an effective $\gamma \sim 1/\sqrt{N} \sim 0.02$ which is only at the beginning of the decay with the exponent ν_D shown in Fig. 12(right panel), if we assume a simple relation $\gamma = K$, which however still may have an additional numerical factor. It is interesting to note that the case with $\nu_D = 0$ corresponds to independence of D on N after rescaling that is the case for nonlinear model C44 (with both potentials having power 4 in (3)) where the spreading goes indeed with the exponent $\alpha = 8/9$ as it is shown in [40].

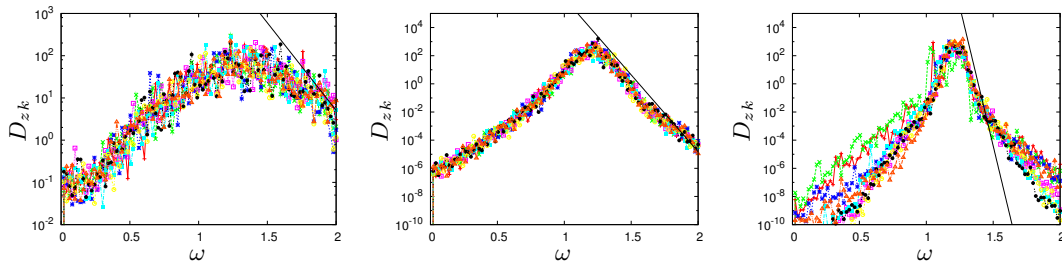


Fig. 14 Diffusion $D_{zk}(\omega)$ in z -variable for particles $k = 1, \dots, 8$, shown by different color symbols, in model C1 at $L = 8$ and $\gamma = 1.0965 \cdot 10^{-2}$ (left), $1.5849 \cdot 10^{-3}$ (middle), $1.2023 \cdot 10^{-4}$ (right). The straight line shows the dependence $D_{zk} \propto \exp(-\omega/\sqrt{\gamma})$.

An indirect support to the view point according to which at $t_{max} = 10^8$ we still did not reach the asymptotic spreading exponent $\alpha = 0.3636$ is based on the numerical computation of the diffusion rate in an additional effective degree of freedom described by the equation $dz_k/dt = q_k \sin(\omega t)$, where q_k are dynamical variables in model C1 (3). Solving these equations in parallel with the dynamical equations of motion for q_k we determine the effective diffusion constant $D_{zk}(\omega)$ for each particle k at $L = 8$. To suppress regular quasiperiodic oscillations we use the window averaging method described in [43] computing first the average $\bar{z}_k(j) = \int_{jT}^{(j+1)T} z_k(t) \sin^6(2\pi t/T) dt / \int_{jT}^{(j+1)T} \sin^6(2\pi t/T) dt$ over time interval $T = 10^6$ and determining the diffusion for each k via the relation $D_{zk}(\omega) = \sum_{j' > j \geq 1} (\bar{z}_k(j) - \bar{z}_k(j'))^2 / ((j' - j)T)$. The computation is done for one trajectory with total time $t = 10^7$. The initial particle energies are chosen to be $E_k = p_k^2/2 + q_k^4/4 \approx 1$ at $q_k = 0$. At $\gamma = 0$ we have the particle action $I_k = \Gamma(1/4)E_k^{3/4} / (2\sqrt{\pi}\Gamma(7/4))$ and nonlinear frequency $\omega_k = \partial H / \partial I_k = 8\sqrt{\pi}\Gamma(1/4)E_k^{1/4} / (3\Gamma(7/8)) \approx$

$1.2E_K^{1/4} \approx 1.2$. The dependence of D_{zk} on frequency ω is shown in Fig. 14 for all k values. In fact, $D_{zk}(\omega)$ gives us the spectral density of an effective noise produced by dynamical chaos. According to the results obtained for the modulational diffusion [43], the spectrum of $D_{zk}(\omega)$ is expected to have a plateau of width $\Delta\omega$ centered at the resonance $\omega_k \approx 1.2$, followed by an exponential drop $D_{zk}(\omega) \propto (1/\Delta\omega) \exp(-|\omega - \omega_k|/\Delta\omega)$. In the picture of triplet resonance we have $\Delta\omega \sim \sqrt{\gamma}$. The data of Fig. 14 are in a satisfactory agreement with such a picture showing a decrease of the plateau size with the decrease of γ . The plateau is followed by an exponential drop. However, at $\gamma \sim 0.01$ the spectral width $\Delta\omega$ is still rather large being comparable with $\omega_k \sim 1$. At such spectral width even the oscillators that are not directly involved in the triplet resonance still will be affected by it. This is probably the reason why up to $\gamma \sim 0.02$ we have the spreading of chaos with the exponent $\alpha \approx 0.6$ corresponding to a usual diffusion $D \propto \gamma^2$ in model C2. At $\gamma \sim 10^{-4}$ the spectral width becomes notably smaller than unity but one needs to go to enormously large times $t_{max} \sim 10^{26}$ to reach such effective values of γ during spreading of chaos. The value $K \sim \gamma \sim 10^{-5}$ where there is a change in the dependence $D(K)$ detected by Chirikov and Vecheslavov (see Fig. 1 in [11]) would require times at least as large as $t_{max} \sim 10^{33}$. Definitely such times remain out of reach of modern computations.

On the basis of presented results and discussions we can say that the spreading of chaos over the nonlinear oscillator lattice of model C2 (3) goes in a subdiffusive way (15) with the exponent $\alpha \approx 0.55$ up to times $t \sim 10^8$. In view of the result of Chirikov and Vecheslavov for the fast Arnold diffusion (13) [11] it is possible that the exponent will go down to $\alpha \approx 0.36$ at times $t > 10^{26}$. The properties of chaos spreading behind times 10^{33} remain absolutely unknown. During this anomalous slow growth of the wave packet size, the chaotic spreading follows the Arnold web of tiny chaotic layers propagating mainly along mostly thick ones. However, from time to time a trajectory can go inside thinner layers that leads to a strong drop of local diffusion and propagation rates, as well as a significant drop of LE (see, e.g., Fig. 9). It is quite possible that in this regime the energy E_k distribution over the populated modes $N(t)$ is still more or less homogeneous, as it is seen in Fig. 13, however, we expect this state to be not ergodic within these N modes since chaos is presumably confined inside some ‘‘porous medium’’ of Arnold web with very complex structure and topology. In course of spreading, the energy per excited oscillator goes down to zero, so that such a process can be considered as an unusual non-ergodic cooling.

7 Slow diffusion in Hamiltonian systems as deterministic rheology

The spreading of chaos discussed above goes in a very slow way. In this section we explore a parallel with slow rheology processes characterized by small values of the Deborah number [44]

$$D_R = t_r/t_{obs} \sim 1/(\lambda t_{obs}) \ll 1, \quad (16)$$

where t_r is a time scale of local relaxation process and t_{obs} is a time of observation. The values of $D_R \ll 1$ correspond to a liquid-like phase while $D_R \gg 1$ appears for the solid phase. At our initial state with one or few excited oscillators we have the relaxation time to be comparable with the inverse LE $t_r \sim 1/\lambda \sim 1$, while the observation time of spreading is $t_{obs} \sim 10^8$ for our numerical simulations. Thus we have extremely small values of $D_R \sim 10^{-8}$ for our studies. The parallels with rheology processes, which are actively studied in soft matter and porous materials (see e.g [45, 46]), can be build on the basis of the following arguments: a) in rheology the flow processes are characterized by small D_R values that is exactly the case for chaos spreading in model C2; b) often a spreading in a porous media is described by a nonlinear diffusion for a density $\rho(x, t)$ [47]:

$$\partial\rho/\partial t = D_0\partial(\rho^a\partial\rho/\partial x)/\partial x \quad (17)$$

and it was shown recently that this equation gives a good phenomenological description of chaos spreading in nonlinear lattices; [26]; c) the Arnold web of chaotic resonance layers forms some kind of a porous media along which energy can spreads to larger and larger sizes. Recent experiments on gel formed by attractive colloidal hard spheres, suspended in an aqueous solvent, show that the spreading of gel is indeed well described by such type of a nonlinear diffusion equation (17) with a nonlinear flux term [48]. The theoretical models of rheology flow try to explain such a spreading by phenomenological statistical models with disorder and metastability (see e.g. [49, 50]). In contrast to such statistical models, our ‘‘rheology’’ of chaos spreading has purely dynamical and deterministic origin.

The value of D_R given above should be considered as a global simplified estimate. It is also important to see how D_R varies with time t_{obs} of spreading duration. For the model C2 we have $\lambda \sim I_k \sim E_k^{3/4} \sim N^{-3/4} \sim t_{obs}^{-3\alpha/8}$ and hence from (16) we find $D_R(t) \sim 1/t_{obs}^{1-3\alpha/8} \propto 1/t_{obs}^{0.78} \gg 1$. Thus in this model $D_R \rightarrow 0$ at $t_{obs} \rightarrow \infty$ that argues in a favor of continuation of spreading at infinitely large times. The same criterion applied to the DANSE model, which describes the Anderson model with nonlinearity $\beta|\psi|^2$ and was studied in [18], gives $\lambda \sim I \sim \beta/N \sim \beta/t_{obs}^{\alpha/2}$ and thus $D_R \sim 1/(\beta t_{obs}^{(1-\alpha/2)})$ still goes to zero in the limit of large times ($\alpha \approx 1/3$ for DANSE). The above arguments show that for the nonlinearity $\beta|\psi|^{2a}$ studied in [26] we have $\lambda \sim I^a \sim 1/t_{obs}^{\alpha a/2}$ and $D_R \sim 1/t_{obs}^{(1-\alpha a/2)} \rightarrow 0$ even for $a = 2, 3$ (see corresponding values of α given in [26]). Indeed, the numerical results of [26] show an infinite spreading for such values of a .

The above discussion shows that weakly nonintegrable many-body Hamiltonian systems give a new interesting example of rheology of chaotic dynamics. These systems are ruled by purely deterministic and rather simple Hamiltonian equations of motion. Exploring further statistical properties of such a deterministic rheology, generated by Hamiltonian many-body dynamics, is an important task for future studies.

8 Conclusion

In this paper we studied properties of non-integrable Hamiltonian lattices focusing on the regimes of very weak non-integrability. Our main results are scaling relations for the probability to observe strong chaos with the largest possible Lyapunov exponent. This probability is proportional to the product of the coupling parameter and the lattice length, while the Lyapunov exponent scales as a square root of the coupling constant. This behavior is explained by the observation that strong chaos is mainly due to resonances that appear when three neighboring sites occasionally have close frequencies. Because both the frequency mismatch and the characteristic time scale of the resonance are proportional to a square root of the perturbation parameter, the relations above directly follow from this scaling.

Furthermore, we confirm previous calculations showing that the diffusion time scale at weak non-integrability is much larger than the inverse Lyapunov exponent, and relate this to a weak diffusion inside the weak chaos component. The measure of this component decreases only algebraically with the strength of nonlinear coupling between nonlinear oscillators. The obtained results are in a good agreement with the fundamental finding of Chirikov and Vecheslavov [9,10,11] who first discovered this regime, with only algebraic decrease of the measure of chaos and diffusion rate at rather small perturbations, and named it the fast Arnold diffusion.

We also studied the spreading of chaos in such coupled nonlinear lattices showing that the spreading goes in an anomalous subdiffusive way. The link between the exponent of this spreading and the fast Arnold diffusion are also determined.

As already mentioned in the introduction, one has to distinguish weakly nonlinear and weakly non-integrable systems. There is, however, some analogy between the dynamics of weakly nonintegrable lattices studied in this paper and random lattices with weak nonlinearity [28,30,27,18,19]. We consider homogeneous lattices, where resonances appear randomly due to random choice of initial conditions. In random weakly nonlinear lattices resonances are determined by a lattice disorder. So in both cases one can expect that chaos is mainly sitting on resonances. For nonlinear homogeneous lattices, resonances can “move” as the energies on different lattice sites vary, while in weakly nonlinear disordered lattices the resonances are due to disorder and thus are “pinned”. The properties of chaos spreading in the latter case require separate investigations.

Acknowledgements We thank S. Fishman for useful discussions. A.P. thanks UPS, Toulouse for hospitality and support, DLS thanks Univ. of Potsdam for hospitality during visits in 2009, 2010. The work was supported by DFG via grant PI220/12. We thank ZEIK (Univ. Potsdam) and HLRS Stuttgart for providing the computer facilities.

References

1. H. Poincaré, Acta Math. **13**, 1 (1890)

2. B.V. Chirikov, Phys. Rep. **52**, 265 (1979)
3. A.J. Lichtenberg, M.A. Lieberman, *Regular and Chaotic Dynamics* (Springer, New York, 1992)
4. V.I. Arnold, Dokl. Akad. Nauk SSSR **156**, 9 (1964).
5. B.V. Chirikov, *Research concerning the theory of non-linear resonance and stochasticity*, Report 267, Inst. of Nuclear Phys., Novosibirsk (1969) [English CERN Trans. 71-40, Geneva (1971)].
6. N.N. Nekhoroshev, Usp. Mat. Nauk **32**(6), 5 (1977).
7. P. Lochak, Uspekhy Mat. Nauk (Russian Math. Surv.) **47**(6), 57 (1992).
8. V. Kaloshin and M. Levi, SIAM Review **50**(4), 702 (2008).
9. B.V. Chirikov and V.V. Vecheslavov, *KAM integrability*, in *Analysis, et cetera* Eds. P.H. Rabinowitz and E. Zehnder, Research papers published in honor of Jurgen Moser's 60th birthday, Academic Press, Inc., N.Y. p.219 (1990).
10. B.V. Chirikov and V.V. Vecheslavov, J. Stat. Phys. **71**, 243 (1993).
11. B.V. Chirikov, V.V. Vecheslavov, Sov. Phys. JETP **85**(3), 616 (1997) [Zh. Eksp. Teor. Fiz. **112**, 1132 (1997)].
12. E. Fermi, J. Pasta, S. Ulam, and M. Tsingou, Los Alamos Report No. LA-1940, 1955 (unpublished); E. Fermi, Collected Papers, University of Chicago Press, Chicago, 1965, Vol. 2, p. 978.
13. A focus issue on "The "Fermi-Pasta-Ulam" problem – the first 50 years" (ed. by D. K. Campbell, P. Rosenau and G. Zaslavsky), CHAOS **15**(1) (2005)
14. G. Gallavotti (ed.), *The Fermi-Pasta-Ulam problem* (Springer Lecture Notes in Physics vol. 728, 2008)
15. G. Benettin, R. Livi, A. Ponno, J. Stat. Phys. **135**(5-6), 873 (2009)
16. D.L. Shepelyansky, Phys. Rev. Lett. **70**, 1787 (1993).
17. M.I. Molina, Phys. Rev. B **58**(19), 12547 (1998)
18. A.S. Pikovsky, D.L. Shepelyansky, Phys. Rev. Lett. **100**(9), 094101 (2008)
19. I. Garcia-Mata, D.L. Shepelyansky, Eur. Phys. J. B **71**(1), 121 (2009)
20. S. Flach, D.O. Krimer, C. Skokos, Phys. Rev. Lett. **102**(2), 024101 (2009)
21. C. Skokos, D.O. Krimer, S. Komineas, S. Flach, Phys. Rev. E **79**(5, Part 2), 056211 (2009)
22. M. Mulansky, K. Ahnert, A. Pikovsky, D.L. Shepelyansky, Phys. Rev. E **80**, 056212 (2009)
23. Ch. Skokos, S. Flach, Phys. Rev. E **82**(1), 016208 (2010)
24. S. Flach, Chem. Physics **375**(2-3), 548 (2010)
25. T.V. Laptyeva, J.D. Bodyfelt, D.O. Krimer, Ch. Skokos, S. Flach, Europhys. Lett. **91**(3), 30001 (2010)
26. M. Mulansky, A. Pikovsky, Europhys. Lett. **90**, 10015 (2010)
27. M. Johansson, G. Kopidakis, S. Aubry, Europhys. Lett. **91**(5), 50001 (2010)
28. D.M. Basko. Weak chaos in the disordered nonlinear Schrodinger chain: destruction of Anderson localization by Arnold diffusion. arXiv:1005.5033v1 [cond-mat.dis-nn] (2010)
29. D.O. Krimer, S. Flach, Phys. Rev. E **82**(4, Part 2), 046221 (2010)
30. A. Pikovsky, S. Fishman. Phys. Rev. E **83**, 025201 (2011).
31. W.-M. Wang and Z. Zhang, e-print arXiv:0805.3520 (2008).
32. J. Bourgain and W.-M. Wang, J. Eur. Math. Soc. **10**, 1 (2008).
33. K. Kaneko, T. Konishi, Phys. Rev. A **40**(10), 40 (1989)
34. T. Konishi, K. Kaneko, J. Phys. A **32**, L715 (1990)
35. M. Falcioni, G. Paladin, A. Vulpiani, Europhys. Lett. **10**(3), 201 (1989)
36. M. Falcioni, U. M. B. Marconi, A. Vulpiani, Phys. Rev. A **44**, 2263 (1991)
37. A.J. Lichtenberg, A.M. Aswani, Phys. Rev. E **57**(5), 5325 (1998)
38. E. Ott, *Chaos in Dynamical Systems* (Cambridge Univ. Press, Cambridge, 1992)
39. K. Ahnert and A. Pikovsky, Phys. Rev. E **79**, 026209 (2009).
40. M. Mulansky, K. Ahnert, A. Pikovsky, Phys. Rev. E **83**, 026205 (2011).
41. B.V. Chirikov, D.L. Shepelyansky, Sov. J. Nucl. Fiz. **36**, 908 (1982)
42. D.L. Shepelyansky, Phys. Rev. E **82**, 055202(R) (2010).
43. B.V. Chirikov, M.A. Lieberman, D.L. Shepelyansky, F. Vivaldi, Physica D **14**, 289 (1985).
44. M. Reiner, "The Deborah number", Phys. Today **17**(1), 62 (1964).
45. A. Ya. Malkin, A.I. Isayev, *Rheology: Concepts, Methods, & Applications* ChemTech Publ., Toronto (2006).
46. M.A. Rao, *Rheology of Fluid and Semisolid Foods: Principles and Applications*, Springer, Berlin (2007).
47. G.I. Barenblatt, *Scaling*, Cambridge Univ. Press, Cambridge (2003).
48. G. Brambilla, S. Buzzaccaro, R. Piazza, L. Berthier, L. Cileletti, "Highly nonlinear dynamics in a slowly sedimenting colloidal gel", arXiv: 1102.5172 [cond-mat.soft] (2011) (to appear in Phys. Rev. Lett.)
49. P. Sollich, E. Lequeux, P. Hébraud, M.E. Cates, Phys. Rev. Lett. **78**, 2020 (1997).
50. P. Sollich, *Soft glassy rheology*, in R. G. Weiss, P. Terech (Eds.), *Molecular Gels: Materials with Self-Assembled Fibrillar Networks*, p. 161, Springer, Berlin (2006).